Carcinogenesis vol.32 no.11 pp.1689–1696, 2011
doi:10.1093/carcin/bgr191
Advance Access publication August 22, 2011

Inhibition of chronic pancreatitis and pancreatic intraepithelial neoplasia (PanIN) by capsaicin in *LSL-Kras^{G12D}/Pdx1-Cre* mice

Han Bai[1,2], Haonan Li[1], Wanying Zhang[1], Kristina A.Matkowskyj[1], Jie Liao[1], Sanjay K.Srivastava[3] and Guang-Yu Yang[1,*]

[1]Department of Pathology, Feinberg School of Medicine, Northwestern University, 303 East Chicago Avenue, Ward 6-118, Chicago, IL 60611, USA, [2]Department of Infectious Disease, Shengjing Hospital of China Medical University, Shenyang 110004, China and [3]Department of Biomedical Sciences, Texas Tech University Health Sciences Center, Amarillo, TX 79106, USA

*To whom correspondence should be addressed. Tel: +1 312 503 0645; Fax: +1 312 503 0647;
Email: g-yang@northwestern.edu
Correspondence may also be addressed to Sanjay K.Srivastava.
Tel: +1 806 356 4750; Fax: +1 806 356 4770;
Email: sanjay.srivastava@ttuhsc.edu

Capsaicin is a major biologically active ingredient of chili peppers. Extensive studies indicate that capsaicin is a cancer-suppressing agent via blocking the activities of several signal transduction pathways including nuclear factor-kappaB, activator protein-1 and signal transducer and activator of transcription 3. However, there is little study on the effect of capsaicin on pancreatic carcinogenesis. In the present study, the effect of capsaicin on pancreatitis and pancreatic intraepithelial neoplasia (PanIN) was determined in a mutant *Kras*-driven and caerulein-induced pancreatitis-associated carcinogenesis in *LSL-Kras^{G12D}/Pdx1-Cre* mice. Forty-five *LSL-Kras^{G12D}/Pdx1-Cre* mice and 10 wild-type mice were subjected to one dose of caerulein (250 μg/kg body wt, intraperitoneally) at age 4 weeks to induce and synchronize the development of chronic pancreatitis and PanIN lesions. One week after caerulein induction, animals were randomly distributed into three groups and fed with either AIN-76A diet, AIN-76A diet containing 10 p.p.m. capsaicin or 20 p.p.m. capsaicin for a total of 8 weeks. The results showed that capsaicin significantly reduced the severity of chronic pancreatitis, as determined by evaluating the loss of acini, inflammatory cell infiltration and stromal fibrosis. PanIN formation was frequently observed in the *LSL-Kras^{G12D}/Pdx1-Cre* mice. The progression of PanIN-1 to high-grade PanIN-2 and -3 were significantly inhibited by capsaicin. Further immunochemical studies revealed that treatment with 10 and 20 p.p.m. capsaicin significantly reduced proliferating cell nuclear antigen-labeled cell proliferation and suppressed phosphorylation of extracellular signal-regulated kinase (ERK) and c-Jun as well blocked Hedgehog/GLI pathway activation. These results indicate that capsaicin could be a promising agent for the chemoprevention of pancreatic carcinogenesis, possibly via inhibiting pancreatitis and mutant *Kras*-led ERK activation.

Introduction

Chronic pancreatitis is a well-recognized risk factor for pancreatic cancer (1). In the process of long-standing chronic inflammation, overproduction of reactive oxygen species and nitrogen species (2), aberrant arachidonic acid metabolites and overproduction of cytokines or growth factors as well their activated signaling pathways may contribute to carcinogenesis (3). These crucial inflammatory processes may cause genetic damage or interact with genetic susceptible genes, further leading to carcinogenesis, such as oncogenic *Kras* gene mutation in pancreatic cancer (4). Thus, targeting pancreatitis and its related key molecular events would be significant for the prevention of pancreatic carcinogenesis.

Capsaicin (trans-8-methyl-*N*-vanillyl-6-nonenamide) is a major active ingredient found in chili peppers. Capsaicin is a water-insoluble derivative of homovanillic acid; chemically, it is an acylamide of homovanillic acid presenting three functional moieties: vanillyl, acylamide and alkenyl (5). Biologically, capsaicin is a TRPV1 agonist. TRPV1, a transient receptor potential cation channel, subfamily V member 1, resides on the membranes of pain- and heat-sensing neurons. When capsaicin binds to the TRPV1 protein, it activates the calcium channel, resulting in the feeling of pain and heat (6). Chronic exposure to capsaicin results in depletion of neurotransmitters (substance P) in neurons and blockade of neurogenic inflammation (7).

Extensive *in vitro* studies indicate that capsaicin is a cancer-suppressing agent that inhibits cell proliferation and induces cell apoptosis. Thoennissen *et al.* (8) have found that capsaicin induces cell cycle arrest and apoptosis in breast cancer cells, mainly via modulating the epidermal growth factor receptor/human epidermal growth factor receptor 2 pathway. Han *et al.* have reported that capsaicin has anti-inflammatory and antitumorigenic activities through blockade of IkB degradation with subsequent inhibition of nuclear translocation of the functionally active nuclear factor-kappaB subunit, p65 and via abolishing phorbol ester-induced activation of activator protein-1 (9). Bhutani *et al.* (10) have found that capsaicin is a novel blocker of interleukin-6 inducible signal transducer and activator of transcription 3 activation in multiple myeloma cells . Other studies indicate that antiproliferation and anticancer actions by capsaicin are possible via modulation of phosphatidylinositol 3-kinases and mitogen-activated protein kinases (MAPK) pathway or through the ubiquitin–proteasome system, E2F pathway (11–13). The anti-inflammatory potential and regulatory effects on xenobiotic metabolism by capsaicin are also noted through its inhibitory effect on inducible COX-2 messenger RNA (mRNA) expression (14) and modulation of cytochrome P450 (CYP 2E1) (15). In addition, the anti-inflammatory action of capsaicin are considered independent of its stimulatory effects on the vanilloid receptors (TRPV1), in which cotreatment with competitive vanilloid receptor inhibitor, capsazepine, does not affect the antiproliferative activity of capsaicin (16).

There are only a few *in vivo* animal studies on determining the chemopreventive effect of capsaicin on carcinogenesis. Anandakumar *et al.* (17) have performed the series of studies on inhibition of benzo(a) pyrene-induced pulmonary tumorigenesis by capsaicin. Capsaicin exhibits its chemopreventive effect through inhibiting carcinogen-induced lung tissue damage and cell proliferation, modulating pulmonary antioxidant defense systems and stabilizing pulmonary mitochondrial enzyme systems. Another study demonstrates a significant inhibitory effect of capsaicin on mutagenesis and/or covalent DNA binding of aflatoxin B1 and tobacco-specific nitrosamine 4-(methylnitrosamino)-1-(3-pyridyl)-1-butanone (NNK) (18).

Oncogenic *Kras* mutation is one of the most common genetic abnormalities in precancerous lesions of the pancreas and pancreatic ductal adenocarcinomas (19). There has been great progress in using genetically engineered mice to generate molecular mimicry models of pancreatic adenocarcinomas (20,21). The *Lox-STOP-Lox* (*LSL*) construct is inserted into the mouse genomic *Kras* locus upstream of a modified exon 1 engineered to have a G→A transition at codon 12 (22,23). To study the role of the mutant *Kras* gene in the initiation of pancreatic carcinogenesis, expression of the mutant allele specifically in the pancreatic epithelial cells is achieved by crossing *LSL-Kras^{G12D}*

Abbreviations: cDNA, complementary DNA; ERK, extracellular signal-regulated kinase; IHC, immunohistochemical; MAPK, mitogen-activated protein kinase; MPO, myeloperoxidase; mRNA, messenger RNA; PanIN, pancreatic intraepithelial neoplasia; PCNA, proliferating cell nuclear antigen; PCR, polymerase chain reaction; PDGF, platelet-derived growth factor; PI, proliferative index; TGF, transforming growth factor.

mice with Pdx1-Cre mice that express Cre-recombinase from the pancreatic-specific promoter, Pancreatic and duodenal homeobox 1 (PDx1) (24). In *LSL-Kras^{G12D}/Pdx1-Cre* mice at age of 5 months, the majority of ducts in pancreas are normal; by 7–10 months, >80% of the animals develop pancreatic intraepithelial neoplasias (PanINs) lesions (predominantly PanIN-1A and 1B lesions) and a few of these lesions are high-grade PanIN-2 and -3; rare carcinomas are observed. To further study, chronic pancreatitis and *Kras* gene mutation in pancreatic carcinogenesis, a mutant *Kras*-driven and caerulein-induced pancreatitis-associated carcinogenesis has been studied in *LSL-Kras^{G12D}/Pdx1-Cre* mice (25) and shows a significantly enhanced development of pancreatitis and cancer. Caerulein is a cholecystokinin analog that is commonly used to induce either acute or chronic pancreatitis. The induction of pancreatitis by caerulein depends on the schedule and dose used (26,27).

Capsaicin has shown a protective effect on xylazine and ketamine hydrochloride-induced acute pancreatitis in rats (28). In the present study, using a mutant *Kras*-driven and caerulin-induced pancreatitis-associated carcinogenesis model in *LSL-Kras^{G12D}/Pdx1-Cre* mice, the effect of capsaicin on chronic pancreatitis and murine pancreatic intraepithelial neoplasia (mPanIN) was examined. Histopathologic and immunohistochemical (IHC) analysis was further performed to evaluate chronic pancreatitis, mPanIN lesions and mutant *Kras*-related signals. Quantitative real-time polymerase chain reaction (PCR) was further used to analyze the transcriptional expression levels of transforming growth factor β (TGF-β), platelet-derived growth factor β (PDGF-β) and the activation of sonic hedgehog (Shh) and GLI1 in the pancreatic tissues.

Material and methods

Reagents

Capsaicin (purity ≥95% by high-performance liquid chromatography) and caerulein (purity ≥97% by high-performance liquid chromatography) were purchased from Sigma–Aldrich (St Louis, MO). Antibody against myeloperoxidase (MPO) was obtained from Abcam (Cambridge, MA), antibody against proliferating cell nuclear antigen (PCNA) was purchased from Calbiochem (Merck KGaA, Darmstadt, Germany). Rat anti-murine Mac-3 monoclonal antibody was obtained from Novus Biologicals (Littleton, CO). Rabbit monoclonal antibodies against phosphor-p44/42 MAPK [extracellular signal-regulated kinase (ERK1/2)], p44/42 MAPK (ERK1/2), phosphor-MEK1/2 and MEK1/2 were from Cell Signaling Technology (Boston, MA). Anti-c-KRas (Ab-1) mouse monoclonal antibody was from Calbiochem—(Merck KGaA). Anti-flotillin-2 (B-6) antibody was from Santa Cruz Biotechnology (Santa Cruz, CA). AIN-76A diet and AIN-76A capsaicin-supplemented diets were from Research Diets (New Brunswick, NJ).

Animals

Six-week-old breeding pairs of *Pdx1-Cre* and *LSL-Kras^{G12D}* mice were used. *Pdx1-Cre* mice were kindly provided by Dr Lowy (University of Cincinnati). *LSL-Kras^{G12D}* mice were obtained from MMHCC, NCI/NIH and kindly provided by Dr T Jacks (MIT). All of the mice are C57BL/6J background through more than five generation backcross with C57BL/6J mice. All of these genetically engineered mice were bred and genotyped in our lab following the protocols provided by the investigators (29). To produce compound transgenic *LSL-Kras^{G12D}/Pdx1-Cre* mice, *LSL-Kras^{G12D}* mice were mated with heterozygous *Pdx1-Cre* transgenic mice. Mice were housed under pathogen-free conditions in the facilities of Laboratory Animal Services, Northwestern University. All studies were conducted in compliance with the Northwestern University IACUC guidelines.

Animal experiments

Four-week-old *LSL-Kras^{G12D}/Pdx1-Cre* mice ($n = 45$) and wild-type C57BL/6J mice ($n = 10$) were subjected to one dose (250 μg/kg body wt) of caerulein using an intraperitoneal injection to induce and synchronize the development of chronic pancreatitis, according to the published method with modification (25). The mice were randomly distributed into three groups ($n = 15$ mice per group), including Group 1 which was fed AIN-76A diet alone, Group 2 was fed AIN-76A diet supplemented with 10 p.p.m. capsaicin and Group 3 was fed AIN-76A diet supplemented with 20 p.p.m. capsaicin. Doses of capsaicin were established based on a review of the literature (16). The diets were replenished every 3–4 days. To avoid any potential interaction between capsaicin and caerulein, capsaicin diet proceeds 1 week following pancreatitis induction and will continue until termination of the experiment. Animals received 8 weeks of capsaicin supplementation in their diet (Groups 2 and 3 only). Food and water consumption were monitored every other day and body weight was measured weekly.

Tissue processing and histological analysis of chronic pancreatitis and mPanIN lesions

After killing, the mice by CO_2 asphyxiation, pancreata and other key organs (including liver and spleen, etc) were collected and weighed. The tissues were then fixed in 10% formalin for 24 h, routinely processed and embedded in paraffin. Serial paraffin sections (5 μm) were made and stained with hematoxylin and eosin for histopathological examination. Additional tissue sections were obtained on poly-L-lysine coated slides for histochemical staining (Masson Trichrome and Alcian blue) and IHC analyses.

Chronic pancreatitis was analyzed and graded using a semiquantitative scoring system according to the established criteria in the literature. The stained slides were blinded to the treatment group for the pathologist's review (30). Briefly, the chronic pancreatitis index was expressed as a sum of scores on loss of acini, extent of inflammatory cell infiltration and stromal fibrosis. Pathologic grading was as follows: (i) extent or areas of loss of pancreatic acini were graded as 0, absent; 1, <10%; 2, 10–30%; 3, 30–50% and 4, >50% of the pancreas area; (ii) number of inflammatory cells per high power field (×40 objective lens) was measured for at least 10 non-overlapping and randomly selected fields and graded as 0, absent; 1, 1–30; 2, 31–50; 3, 51–100 and 4, >100 cells and (iii) the area and intensity of stromal fibrosis was graded as 0, absent; 1, <5%; 2, 5–10%; 3, 10–20%; 4, >20% fibrosis of the pancreas based on Masson's Trichrome staining.

Murine pancreatic intraepithelial neoplasia (mPanIN) was analyzed based on the established criteria (31) and was graded as: mPanIN-1, mPanIN-2 and mPanIN-3.

Immunohistochemistry

IHC staining was performed according to our routine protocol using an avidin–biotin–peroxidase method (32). Sections were deparaffinized and rehydrated. Antigen unmasking solution was used to retrieve the antigens. The sections were quenched with 3% hydrogen peroxidase and blocked with normal horse serum. The sections were then incubated with anti-MPO (1:35), anti-Mac-3 (1:50), anti-PCNA (1:80) or anti-phospho-ERK1/2 (1:100) in antibody incubating solution. After incubation with the appropriate biotinylated secondary-antibody (mouse or rabbit) using the ImmPRESS reagent kit, a characteristic brown color was developed by incubation with 3,3-diaminobenzidine substrate chromogen system (Sigma–Aldrich). Specific antibody-labeled signals were analyzed using a Nikon bright field research microscope along with appropriate negative and positive controls.

Protein extraction and western blot assay

Freshly harvested pancreas was homogenized and lysed in ice-cold RIPA lysis buffer (Santa Cruz Biotechnology) containing 1% phosphatase inhibitor cocktail 1 and 2, 2% protease inhibitor cocktail, 1% phenylmethyl sulfonylfluoride and 1% sodium orthovanadate for 60 min by vortexing every 5 min. The lysates were separated by centrifugation at 12 000*g* for 5 min at 4°C; the supernatants were collected, aliquoted and stored at −80°C. Membrane proteins from pancreatic tissues were extracted using Mem-PER Eukaryotic Membrane Protein Extraction Reagent Kit (Thermo Scientific, Waltham, MA) according to manufacturer's instructions. All protein concentrations were determined using Bradford reagent (Thermo Scientific) per the manufacturer's instructions.

An aliquot (20 μg protein per lane) of the total protein was separated by 12% sodium dodecyl sulfate–polyacrylamide gel electrophoresis gel for Kras or 10% sodium dodecyl sulfate–polyacrylamide gel electrophoresis gel for phospho-ERK or ERK and phosphor-MEK or MEK and transferred onto a polyvinylidene fluoride membrane. After blocking with 5% bovine serum albulin in 1× Tris-buffered saline with 0.1% Tween-20 (TBST) or 5% non-fat milk in TBST, the membranes were incubated with the primary antibody overnight at 4°C. The primary antibodies included KRas (Ab-1) (1:20), flotillin-2 (1:100), Phospho-p44/42 MAPK (Erk1/2) (Thr202/Tyr204) (20G11) (1:1000), p44/42 MAPK (Erk1/2) (1:1000), Phospho-MEK1/2 (Ser221) (166F8) (1:1000) and MEK1/2 (1:1000). The membrane was further incubated with horseradish peroxidase-linked anti-rabbit IgG or anti-mouse IgG and horseradish peroxidase-linked anti-biotin antibodies for 1 h at room temperature. Between steps, the membrane was washed with 1× TBST. The protein–antibody complexes were detected using a chemiluminescent substrate according to the manufacturer's instructions and the emitted light captured on X-ray film.

RNA extraction and quantitative reverse transcript-PCR assay

Total RNA was extracted from the freshly collected pancreas tissues using the RNeasy kit (Qiagen, Valencia, CA). First-strand complementary DNA (cDNA)

was synthesized using 1 μg of total RNA in a 20 μl reverse transcriptase reaction mixture using iScript™ cDNA Synthesis Kit (Bio-Rad, Hercules, CA) according to the manufacturer's instructions. The region of TGF-β, PDGF-β, SHH and GLI1 mRNA were amplified using primers TGF-β (forward 5′-TTGCTTCAGCTCCACAGAGA-3′; reverse 5′-TGGTTGTAGAGGGCAAGGAC), PDGF-β (forward 5′-CCCACAGTGGCTTTTCATTT-3′; reverse 5′-GTGGAGGAGCAGACTGAAGG-3′), SHH (forward 5′-CCTCTCCTGCTATGCTCCTG-3′; reverse 5′-GTGGCGGTTACAAAGCAAAT-3′), GLI1 (forward 5′-ACTAGGGGGCTACAGGAGGA-3′; reverse 5′-ACCTGGACCCCTAGCTTCAT-3′) designed using the primer 3 software. Glyceraldehyde-3-phosphate dehydrogenase (GAPDH) was used as the internal control (forward 5′-GCACAGTCAAGGCCGAGAAT-3′; reverse 5′-GCCTTCTCCATGGTGGTGAA-3′). All real-time PCR reactions were performed in a 20 μl mixture containing 1.5 μl cDNA preparation, 10 μl SYBR Green buffer (Bio-Rad), 0.4 μM of each primer, 7.7 μl DEPC water (diethylprocarbonate) (Bio-Rad). Real-time quantitation was performed using the Mini-iOpticon Real-Time PCR System (Bio-Rad). PCR conditions were: 50°C for 2 min, 95°C for 2 min, followed by 40 cycles of 95°C, 15 s; 58°C, 3 s and 50°C, 1 s. Data of each mRNA expression were shown as the relative folds of change normalized by that of GAPDH.

Statistical analysis

Each analyzed parameter is expressed as mean ± SD, unless otherwise stated. Continuous variables were compared with the Student's *t*-test, whereas categorical variables were compared with Chi-square test. All statistical tests were two sided, and statistical significance was taken as $P < 0.05$.

Results

General animal data

LSL-Kras^{G12D}/Pdx1-Cre mice fed AIN-76A or capsaicin diets had steady body weight gains. As shown in Table I, there was no significant difference of body weight in the mice fed either AIN-76A or AIN-76A diets supplemented with either 10 or 20 p.p.m. capsaicin. None of the animals fed the capsaicin diets exhibited any observable toxicity or any gross morphologic changes to liver, spleen, kidney or lung. There were also no differences in the amount of water or food consumption among the treatment and control mice.

Effect of capsaicin diet on pancreas weight and chronic pancreatitis in LSL-Kras^{G12D}/Pdx1-Cre mice

Pancreatic weight is a simple marker of chronic active pancreatitis. In the C57BL/6J wild-type mice, the average pancreas weight was 0.14 ± 0.04 g. A significant increase in pancreas weight was observed in *LSL-Kras^{G12D}/Pdx1-Cre* mice compared with wild-type mice (0.20 ± 0.04 g, $P < 0.05$). As summarized in Table I, by considering the effect of body weight on the size of pancreas, the ratio of pancreas weight to body weight was further analyzed and revealed a significant difference between wild-type mice and *LSL-Kras^{G12D}/Pdx1-Cre* mice ($P < 0.05$). In *LSL-Kras^{G12D}/Pdx1-Cre* mice fed 10 or 20 p.p.m. capsaicin, the pancreas weights were 0.19 ± 0.03 g and 0.20 ± 0.04 g, respectively, but the difference was not statistically significant from mice fed AIN-76A diet alone ($P > 0.05$). In addition, no significant differences in the weights of the liver and spleen were observed between wild-type mice and *LSL-Kras^{G12D}/Pdx1-Cre* mice fed with either AIN-76A or capsaicin-supplemented diets (Table I).

Extensive histopathologic analysis of the pancreas was performed using hematoxylin- and eosin-stained slides. No microscopic pathologic alteration was observed in wild-type mice fed either AIN-76A or capsaicin-supplemented diets (Figure 1A). In contrast, *LSL-Kras^{G12D}/Pdx1-Cre* mice demonstrated extensive chronic pancreatitis (Figure 1B). The chronic pancreatitis showed a multifocal pattern and was characterized by a loss of acini, terminal ductular proliferation, acinar–ductal mucinous metaplasia, stromal fibrosis and inflammatory cell infiltration (including neutrophils, macrophages, lymphocytes and plasma cells). A marked decrease in the extent of the chronic pancreatitis was observed in mice treated with 10 and 20 p.p.m. capsaicin in their diets (Figure 1C and D).

The chronic pancreatitis was semiquantitatively analyzed based on loss of acinar structure, the intensity of inflammatory cell infiltration and the extent of stromal fibrosis. These parameters were scored using a four-scale system (absent, mild, moderate and severe), and the chronic pancreatitis index was expressed as sum of these scores (scores can range from 0 to 12). As seen Figure 1E, *LSL-Kras^{G12D}/Pdx1-Cre* mice fed 10 or 20 p.p.m. capsaicin-supplemented diets showed significantly decreased chronic pancreatitis index compared with mice fed AIN-76A diet alone (4.39 ± 2.31 or 4.00 ± 1.39 versus 7.11 ± 3.10, $P < 0.05$).

Masson's Trichrome stain highlighted stromal fibrosis in chronic pancreatitis. In pancreatic tissue from wild-type mice, interlobular fibroconnective tissue showed positive staining as demonstrated by a blue color (Figure 1F). Extensive positivity in the pancreatic parenchyma was observed in areas of chronic pancreatitis in *LSL-Kras^{G12D}/Pdx1-Cre* mice (Figure 1G). Markedly decreased stromal fibrosis was observed in *LSL-Kras^{G12D}/Pdx1-Cre* mice fed 10 or 20 p.p.m. capsaicin-supplemented diets (Figure 1H–I). The stromal fibrosis was further semiquantitatively analyzed and showed that the fibrosis score was 2.11 ± 1.04 in *LSL-Kras^{G12D}/Pdx1-Cre* mice fed AIN-76A diet alone and 1.19 ± 0.88 and 1.25 ± 0.43 in *LSL-Kras^{G12D}/Pdx1-Cre* mice fed 10 or 20 p.p.m. capsaicin-supplemented diets, respectively (Figure 1J, $P < 0.05$).

MPO and Mac-3 IHC staining was used to label inflammatory cells (predominantly neutrophils) and macrophages in the pancreas. In pancreatic tissue obtained from wild-type mice, there was no or rare MPO-positive neutrophils and Mac-3-positive macrophages (Figure 1K and P). In contrast, numerous MPO-positive neutrophils and Mac-3-positive macrophages were observed in the pancreas in *LSL-Kras^{G12D}/Pdx1-Cre* mice (Figure 1L and Q), whereas decreased MPO- and Mac-3-positive cells were observed in mice treated with the capsaicin-supplemented diets (Figure 1M, N, R and S). MPO-positive cells per high power field (at ×40 magnification) were further counted (Figure 1O) and revealed that MPO-positive cell numbers were 193.0 ± 88.5 in *LSL-Kras^{G12D}/Pdx1-Cre* mice fed AIN-76A diet alone, whereas a significant reduction of MPO-positive cells was observed in *LSL-Kras^{G12D}/Pdx1-Cre* mice fed a 10 or 20 p.p.m. capsaicin-supplemented diet (30.9 ± 21.2 and 40.0 ± 20.1, respectively, $P < 0.05$). Similarly, as seen in Figure 1T, Mac-3-labeld macrophages were further semiquantitated and showed that Mac-3-positive cell numbers were 73.2 ± 16.7 in *LSL-Kras^{G12D}/Pdx1-Cre* mice fed AIN-76A diet alone, whereas a significant reduction of Mac-3-positive cells was found in *LSL-Kras^{G12D}/Pdx1-Cre* mice fed a 10 or 20 p.p.m. capsaicin-supplemented diet (35.5 ± 12.4 and 31.5 ± 15.0, respectively, $P < 0.05$).

Inhibition of mPanIN lesion formation and progression by capsaicin

All of *LSL-Kras^{G12D}/Pdx1-Cre* mice fed either AIN-76A diet alone or capsaicin-supplemented diets developed pancreatic acinar–ductal mucinous metaplasia or mPanIN-1 lesions (Figure 2A). But, a few of the mice had mPanIN-2 and mPanIN-3 lesions (Figure 2B and C). The incidences of high-grade mPanIN-2 and mPanIN-3 were 60% (9/15) and 20% (3/15), respectively in *LSL-Kras^{G12D}/Pdx1-Cre* mice fed AIN-76A diet alone. A significant decrease of high-grade mPanIN lesions was observed in the mice fed 10 or 20 p.p.m. capsaicin-supplemented diets and showed 27% (4/15) and 47% (7/15) for mPanIN-2 and 7% (1/15) and 0% (0/15) for mPanIN-3 lesion, respectively ($P < 0.05$, Figure 2D).

Alcian blue/PAS staining highlighted the intracellular mucin in mucinous metaplasia and mPanINs. Acinar–ductal mucinous metaplasia or mPanIN-1 lesions showed intense alcian blue-positive staining in *LSL-Kras^{G12D}/Pdx1-Cre* mice fed AIN-76A diet alone (Figure 2E) or capsaicin-supplemented diets (Figure 2F and G). The extent of Alcian blue-positive staining within the pancreas was measured semiquantitatively and revealed that positive areas were 9.8 ± 3.0% in *LSL-Kras^{G12D}/Pdx1-Cre* mice fed AIN-76A diet alone and 4.5 ± 2.2% and 6.0 ± 1.8% in *LSL-Kras^{G12D}/Pdx1-Cre* mice fed 10 or 20 p.p.m. capsaicin-supplemented diets, respectively (Figure 2H, $P < 0.05$).

Table I. Body weight and organ weight data from wild-type and *Kras^{G12D}/Pdx1-Cre* mice receiving a capsaicin-supplemented diet or normal control diet

Genotype	Treatment	*n*	Body weight (g)	Pancreas weight (g)	Pancreas/BW[a]	Liver weight (g)	Liver/BW[a]	Spleen weight(g)	Spleen/BW[a]
Pdx1-Cre/Kras^{G12D}	Control	15	24.5 ± 3.8	0.21 ± 0.04	0.009 ± 0.001[b]	1.18 ± 0.26	0.048 ± 0.006	0.13 ± 0.07	0.005 ± 0.002
	Capsaicin 10 p.p.m.	15	24.3 ± 3.6	0.19 ± 0.03[b]	0.008 ± 0.001[b]	1.15 ± 0.20	0.047 ± 0.006	0.09 ± 0.02	0.003 ± 0.001
	Capsaicin 20 p.p.m.	15	23.5 ± 3.8	0.20 ± 0.04[b]	0.008 ± 0.002[b]	1.13 ± 0.22	0.049 ± 0.008	0.10 ± 0.02	0.004 ± 0.001
Wild-type	Control	5	23.0 ± 3.7	0.16 ± 0.04	0.006 ± 0.001	0.94 ± 0.20	0.041 ± 0.005	0.08 ± 0.02	0.003 ± 0.001
	Capsaicin 20 p.p.m.	5	22.6 ± 3.2	0.14 ± 0.04	0.006 ± 0.002	1.07 ± 0.28	0.047 ± 0.006	0.11 ± 0.06	0.004 ± 0.002

[a]Ratio of specific organ to body weight (BW).
[b]Indicating statistically significant differences with $P < 0.05$ in wild-type mice compared with *Kras^{G12D}/Pdx1-Cre* mutant mice.

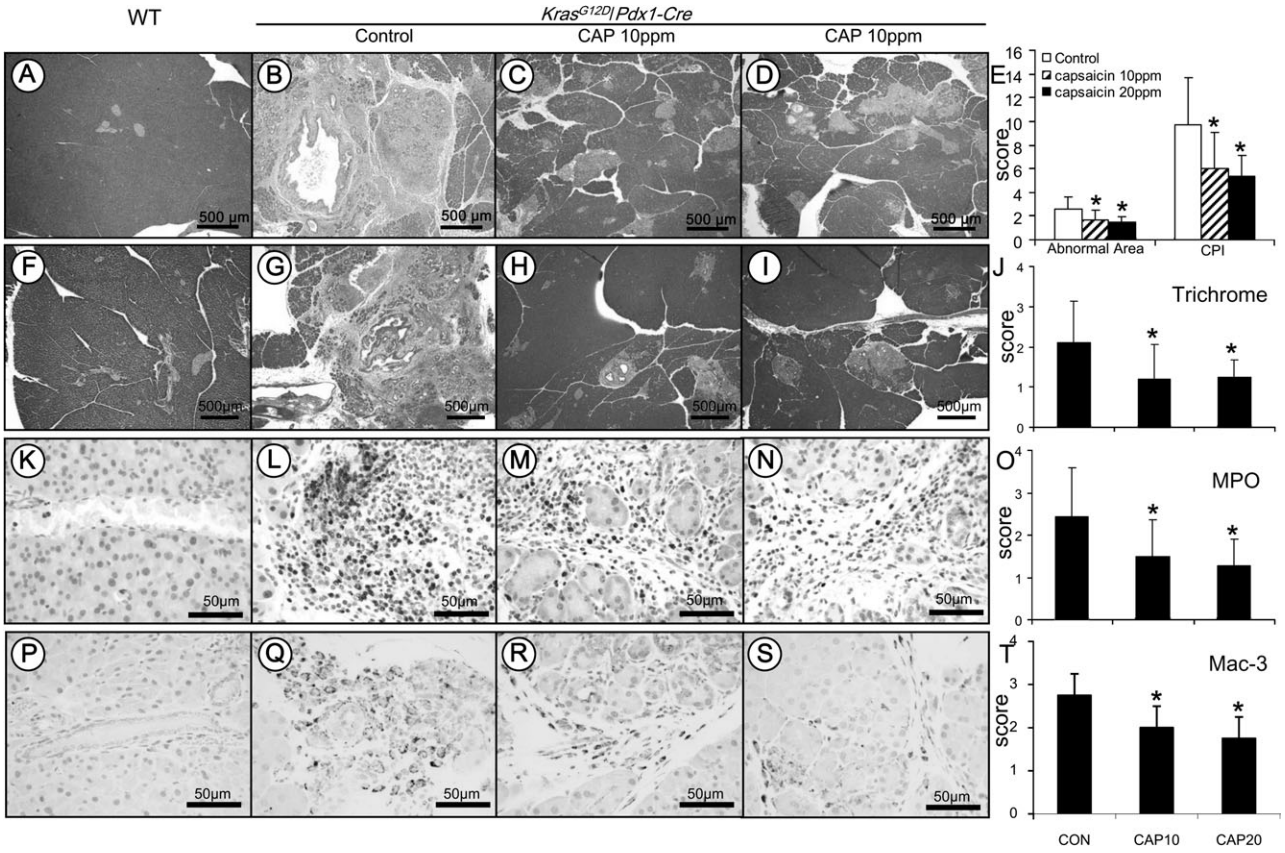

Fig. 1. Analysis of chronic pancreatitis using the approaches of histopathology, immunohistochemistry and histochemistry. Histopathology in the pancreatic tissue of KrasG12D/Pdx1-Cre mice: (**A**) Pancreas in wild-type control mice showing morphologically normal pancreatic parenchyma (acini and islets as well interlobular ducts). (**B**) Extensive chronic pancreatitis in *KrasG12D/Pdx1-Cre* mice fed AIN-76A diet alone showing loss of acini and stromal fibrosis. (**C** and **D**) Minimal to mild chronic pancreatitis in mice fed 10 or 20 p.p.m. capsaicin-supplemented diet, respectively. (**E**) Semiquantitative analysis (histogram) of chronic pancreatitis based on the extent of acinar loss, stromal fibrosis and inflammatory cell infiltration. There was a statistically significant difference in mice fed AIN6A diet alone compared with those given capsaicin-supplemented diets ($P < 0.05$). Trichrome stain highlighting stromal fibrosis in the pancreas: (**F**) Trichrome stained fibroconnective tissue (blue color) only in the interlobular areas of a normal pancreas in wild-type control mice. (**G**) *KrasG12D/Pdx1-Cre* mice fed AIN-76A diet alone showing extensive fibrosis in pancreatic parenchyma. (**H** and **I**) mice fed 10 or 20 p.p.m. capsaicin-supplemented diet exhibiting much less stromal fibrosis in the pancreas. (**J**) Semiquantitative analysis (histogram) of the extent of trichrome stain-labeled stromal fibrosis revealing statistically significant differences in mice fed capsaicin-supplemented diets compared with those given AIN-76A diet alone ($P < 0.05$). MPO-labeled neutrophils in the pancreas: (**K**) Pancreas from wild-type control mice showing no MPO-labeled neutrophils. (**L**) *KrasG12D/Pdx1-Cre* mice fed AIN-76A diet alone displaying intense MPO-labeled neutrophils in the areas of pancreatitis. (**M** and **N**) Mice fed 10 or 20 p.p.m. capsaicin-supplemented diet exhibiting decreased MPO-positive neutrophils. (**O**) Semiquantitative analysis (histogram) of the MPO-labeled inflammatory cells showing a statistically significant difference in mice fed capsaicin-supplemented diets compared with those given AIN-76A diet alone ($P < 0.05$). Mac-3-labeled macrophages in the pancreas: (**P**) Pancreas from wild-type control mice showing no Mac-3-labeled inflammatory cells. (**Q**) *KrasG12D/Pdx1-Cre* mice fed AIN-76A diet alone displaying intense Mac-3-labeled macrophage in the areas of pancreatitis. (**R** and**S**) Mice fed 10 or 20 p.p.m. capsaicin-supplemented diet exhibiting decreased Mac-3-positive macrophages. (**T**) Semiquantitative analysis (histogram) of the Mac-3-labeled macrophages showing a statistically significant difference in mice fed capsaicin-supplemented diets compared with those given AIN-76A diet alone ($P < 0.05$).

Inhibition of PCNA-labeled cell proliferation, phospho-ERK and phospho-c-Jun in chronic pancreatitis and mPanINs by capsaicin

Cell proliferation was measured by PCNA expression in chronic pancreatitis and mPanIN lesions. As shown in Figure 3A–C, markedly decreased PCNA-labeled cells were observed in chronic pancreatitis and mPanIN lesions in *LSL-Kras^{G12D}/Pdx1-Cre* mice fed capsaicin-supplemented diets compared with the pancreatic tissues from *LSL-Kras^{G12D}/Pdx1-Cre* mice fed AIN-76A diet alone. PCNA-labeled cells were measured semiquantitatively and expressed as the percentage of PCNA-labeled cells per total cells counted and referred to as

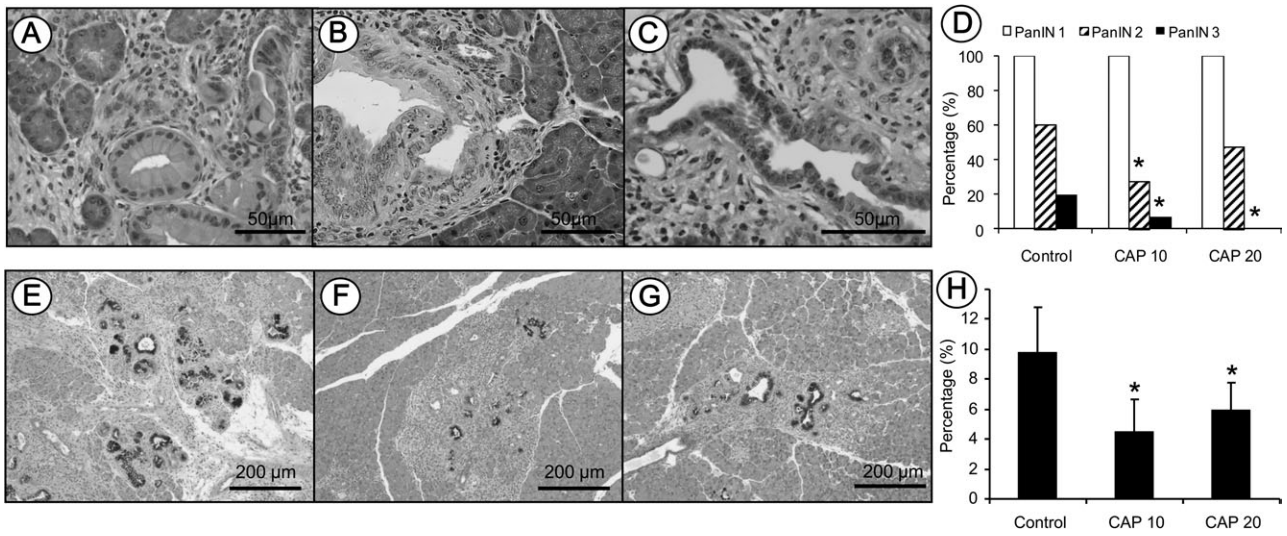

Fig. 2. Histopathological and histochemical analysis of mPanIN lesions in *Kras^{G12D}/Pdx1-Cre* mice. (**A**–**C**) Representative photos of mPanIN-1, mPanIN-2 and mPanIN-3, respectively. (**D**) Semiquantitative analysis (histogram) of mPanIN lesions. Statistically significant lower in the incidence of high-grade mPanIN-2 and mPanIN-3 lesions were observed in mice fed capsaicin-supplemented diets compared with AIN-76A diet alone (Chi-square test, $P < 0.05$). Alcian blue/PAS staining of mucin in mPanIN lesions in (**E**) mice fed AIN-76A diet alone, or (**F** and **G**) mice fed capsaicin-supplemented diets. (**H**) Statistical analysis of PAS/Alcian blue-positive staining areas in the control and capsaicin treatment groups (Chi-square test, $P < 0.05$).

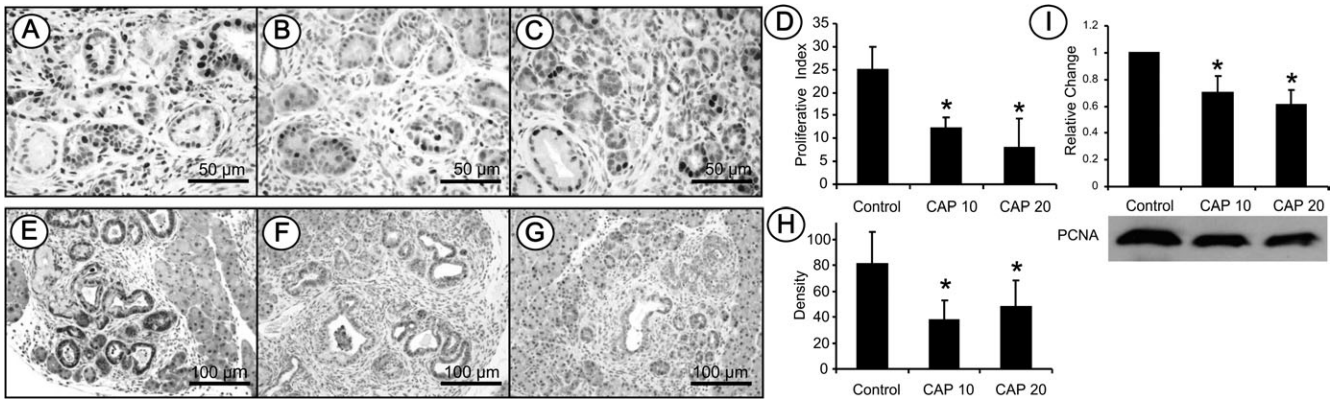

Fig. 3. Immunohistochemistry of PCNA-labeled cell proliferation and phosopho-ERK expression. (**A**) PCNA-labeled cell proliferation in *Kras^{G12D}/Pdx1-Cre* mice fed AIN-76A diet alone. (**B** and **C**) Mice fed capsaicin-supplemented diets. (**D**) Semiquantitative analysis (histogram) of PCNA-labeled cell proliferation. Statistical significance was observed in mice fed capsaicin-supplemented diets compared with those given AIN-76A diet alone ($P < 0.05$). (**E**) Phospho-ERK in *Kras^{G12D}/Pdx1-Cre* mice fed AIN-76A diet alone. (**F** and **G**) Phospho-ERK in mice fed capsaicin-supplemented diets. (**H**) Semiquantitative analysis (histogram) of phospho-ERK staining intensity revealed statistically significant differences in mice fed capsaicin-supplemented diets compared with those given AIN-76A diet alone ($P < 0.05$). (**I**) Western blot of PCNA showing the protein level is statistically lower in the pancreas of *Kras^{G12D}/Pdx1-Cre* mice fed capsaicin-supplemented diets compared with those fed AIN6A diet alone ($P < 0.05$).

the proliferative index (PI). As shown in Figure 3D, PI was 25.0 ± 2.5% in *LSL-Kras^{G12D}/Pdx1-Cre* mice fed AIN-76A diet alone. A significant decrease in the PI was observed in *LSL-Kras^{G12D}/Pdx1-Cre* mice fed 10 or 20 p.p.m. capsaicin-supplemented diet and PI was 12.1 ± 2.5% and 8.0 ± 6.3%, respectively ($P < 0.05$). The expression of PCNA in the pancreas was further analyzed using western blot assay and demonstrated significantly lower PCNA expression in the pancreatic tissue of *LSL-Kras^{G12D}/Pdx1-Cre* mice fed 10 or 20 p.p.m. capsaicin-supplemented diet compared with mice fed AIN-76A diet alone (Figure 3I, $P < 0.05$).

To determine mutant *Kras*-activated signals, phospho-ERK and phospho-c-Jun were analyzed using both immunohistochemistry and western blot approaches. IHC staining showed that acinar–ductal mucious metaplasia or mPanIN lesions were positively labeled by phospho-ERK in *LSL-Kras^{G12D}/Pdx1-Cre* mice fed AIN-76A diet alone (Figure 3E). Markedly decreased phospho-ERK expression was observed in *LSL-Kras^{G12D}/Pdx1-Cre* mice fed a capsaicn-supplemented diet (Figure 3F and G). As shown in Figure 3H, the staining intensity of phospho-ERK was further analyzed semiquantitatively using Image J software and revealed that the staining intensity (OD) was 80.7 ± 24.5 in the mice fed AIN-76A diet alone. A significant reduction in staining intensity for phospho-ERK was found in mice fed 10 and 20 p.p.m. capsaicin-supplemented diet (37.7 ± 14.7 and 47.8 ± 19.9, respectively, $P < 0.05$).

Western blot assay was further performed to quantitatively determine the levels of mutant Kras-activated signals in the pancreatic tissues. As seen in Figure 4A and B, there was no difference in the levels of Kras or phospho-MEK1/2 expression detected in mice treated with capsaicin-supplemented diets when compared with mice fed AIN-76A diet alone. The levels of phospho-ERK and its downstream mediator phospho-c-Jun in pancreatic tissues were significantly decreased in mice treated with capsaicin-supplemented diets ($P < 0.05$), but there was no difference in the levels of non-phosphorylated ERK and c-Jun proteins.

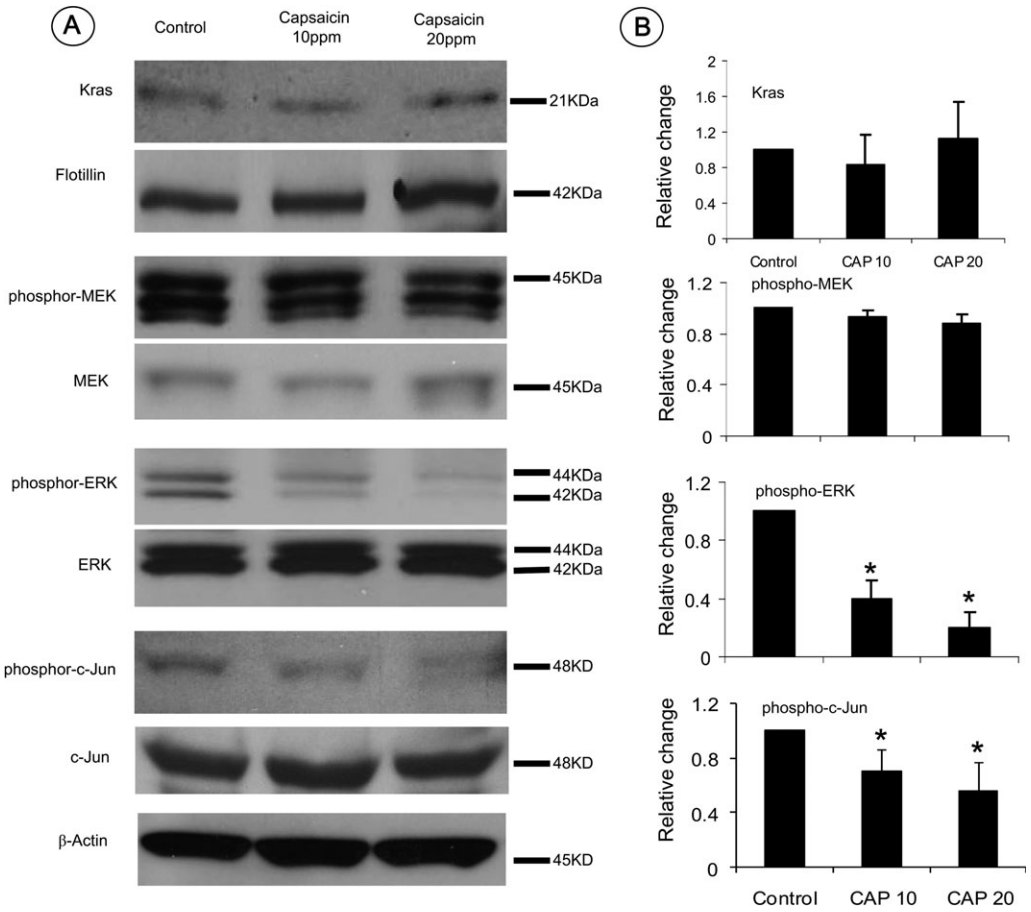

Fig. 4. Western blot assay of mutant Kras and its activated downstream signals phospho-MEK, phospho-ERK and Phospho-c-Jun. (**A**) Expression levels of Kras and its downstream phosphorylated and non-phosphorylated MEK, ERK and c-Jun in the pancreatic tissues detected using a western blot assay. (**B**) Histograms reveal the intensity of expression of membrane-bound Kras and each phospho-protein in mice fed AIN-76A diet alone or capsaicin-supplemented diets ($^{*}P < 0.05$).

Analysis of TGF-β, PDGF-β and active hedgehog signalings using quantitative PCR

Freshly collected pancreatic tissues ($n = 6$ per group, both genders) were analyzed for the fold change of mRNA expression of TGF-β, PDGF-β and active hedgehog signaling Shh and GLI1. Total RNA was isolated and reverse-transcribed into cDNA and quantitated with a real-time PCR assay. As shown in Figure 5, compared with wild-type mice, significantly increased Shh and GLI1 mRNA expressions were observed in the pancreatic tissues of *LSL-KrasG12D/Pdx1-Cre* mice ($P < 0.05$). More than 2-fold decrease of Shh and GLI1 mRNA expressions was found in *LSL-KrasG12D/Pdx1-Cre* mice fed with a diet containing capsaicin in comparison with *LSL-KrasG12D/Pdx1-Cre mice* ($P < 0.05$). Expression of TGF-β and PDGF-β was decreased in *LSL-KrasG12D/Pdx1-Cre* mice fed with a diet containing capsaicin, but it did not reach statistical significance.

Discussion

Clinical evidence indicates that patients with chronic pancreatitis have a 16-fold higher risk of developing pancreatic ductal adenocarcinoma (33). Fresh fruits and vegetables have demonstrated protective effects against inflammation and cancers. There are a wide variety of biologically active components in fresh fruit and vegetables. Capsaicin, the active component in chili peppers, has been shown to have many biological activities including anti-inflammatory and antioxidant functions (34). In the present study, we have demonstrated the chemopreventive effect of capsaicin against pancreatitis and mPanIN lesion formation in a unique genetically engineered pancreatitis model of *LSL-Kras^{G12D}/Pdx1-Cre* mice.

Inflammatory cell infiltration, particularly in neutrophils and macrophages, is the hallmark of an inflammatory process. An intense infiltration of leukocytes overproduce reactive oxygen species, inflammatory mediators such as prostaglandin E2 (PGE_2) and leukotrienes B4 (LTB4), various cytokines and chemokines which contribute to the processes of inflammation and carcinogenesis (35). An increased risk of cancer development has been seen in patients with higher MPO-labeled inflammatory cells (36). Our studies demonstrated a significant decrease in inflammatory cells including neutrophils and macrophages in the pancreas and could be one of key mechanisms inhibiting inflammation and carcinogenesis by capsaicin.

PanIN is the proliferative epithelial precancerous lesion in the small caliber pancreatic ducts (31). Consensus criteria for the diagnosis and grading of mPanINs have been established for models of pancreatic cancer in mice (37). Similar to humans, mPanIN lesions range from low-grade mPanIN (mPanIN-1) to high-grade mPanINs (mPanIN-2 or -3). The initiation and progression of murine PanINs is following the steps from mutant *Kras*-initiated acinar–duct metaplasia to high-grade mPanIN and finally to infiltrating carcinoma (37). In the mutant *Kras*-led and caerulein-induced pancreatitis-associated carcinogenesis in *LSL-Kras^{G12D}/Pdx1-Cre* mice, mPanIN lesions were detected in 100% of the *LSL-Kras^{G12D}/Pdx1-Cre* mice at the age of 13 weeks, with 60% of mice harboring high-grade mPanINs. With capsaicin treatment, high-grade mPanINs was significantly decreased. This result indicates that capsaicin treatment inhibits chronic pancreatitis and thus blocks the progression of high-grade mPanINs.

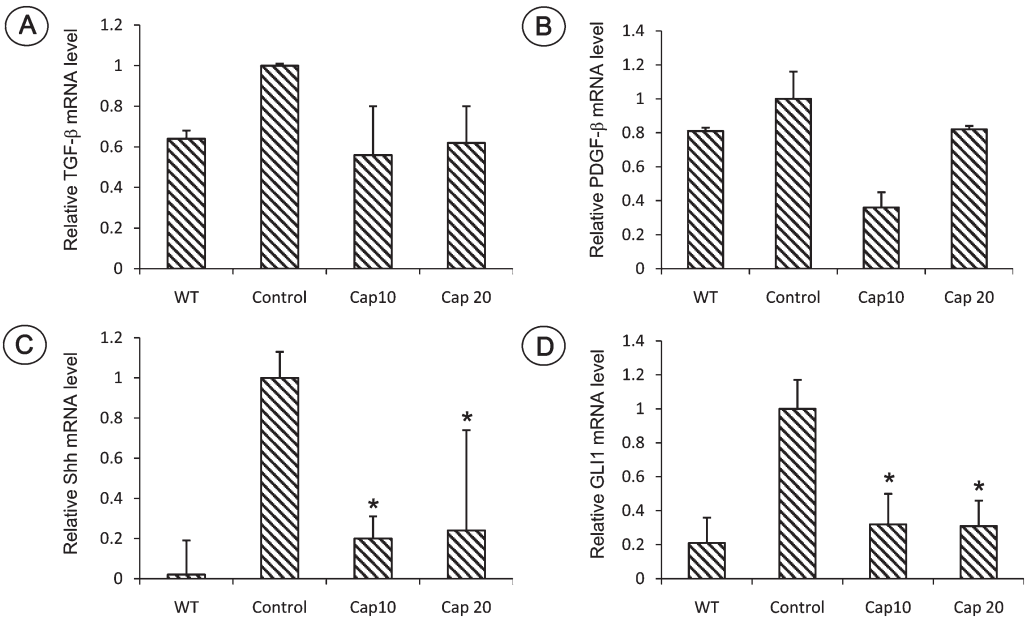

Fig. 5. Quantitative PCR analysis of mRNA expression of TGF-β, PDGF-β, Shh and GLI1 in the pancreatic tissue in wild-type control mice (WT) and *LSL-KrasG12D/Pdx1-Cre* mice fed a diet with or without capsaicin. (**A**) TGF-β; (**B**) PDGF-β; (**C**) Shh and (**D**) GLI1 (*, Significant difference between mice with or without capsaicin treatment, $P < 0.05$).

PCNA is a highly conserved 36 kDa acid nuclear protein, associated with DNA replication and cell proliferation in the mammalian cells. PCNA expression increases at the end of G_1 phase and reaches its maximum in S-phase. It declines during G_2 phase and is absent during the mitotic phase and in quiescent cells. PCNA is widely used as a marker of cell proliferation in various tumors including pancreatic cancers (38). Capsaicin treatment resulted in significantly decreased PCNA-labeled proliferative cells, indicating that inhibition of cell proliferation by capsaicin could be a crucial mechanism for suppressing the progression of mPanINs to carcinoma.

It is well known that the *Ras* gene encodes small guanosine triphosphate-binding cytoplasmic proteins and regulates cell cycle progression mainly via the MAPK and AKT cascade (39). Mutant *Kras* gene is the most common genetic alteration occurring in nearly all pancreatic cancers (28). Mutant *Ras* impairs the intrinsic guanosine triphosphatase activity, leading to persistent activation of Raf/MEK/ERK1/2 that results in cell proliferation and immortalization (40). In *LSL-Kras^{G12D}/Pdx1-Cre* mice, persistent activation of Raf/MEK/ERK1/2, such as phosphorylation of raf, MEK and ERK, were commonly observed in mutant *Kras*-induced mPanIN lesions. We have further investigated the interaction of capsaicin with the oncogenic *Kras*-activated signal transduction pathway. It showed that capsaicin appeared to be a strong inhibitor of phospho-ERK in *LSL-Kras^{G12D}/Pdx1-Cre* mice but did not affect Kras or MEK signal expression. These findings indicate that inhibition of proliferation and carcinogenesis by capsaicin occurs via blocking the aberrant activation of phospho-ERK.

Fibrosis and desmoplasia are some of the main characters of chronic pancreatitis and pancreatic carcinogenesis. Several cytokines such as TGF-β, PDGF-β and the activation of sonic hedgehog (Shh) are closely associated with desmoplasia in chronic pancreatitis and pancreatic cancer (41–43). It has been reported that oncogenic *Kras* is involved in the activation of the hedgehog/GLI pathway, and the crosstalk between Kras and Hedgehog pathway may play an important role in promoting desmoplasia and pancreatic carcinogenesis (44). The effect of capsaicin on pancreatic stroma was evaluated in the current study. Firstly, our results indicated a significant increased Hedgehog/GLI activity in the pancreas of *LSL-Kras^{G12D}/Pdx1-Cre* mice. But, although there were increases of the expression of TGF-β and PDGF-β mRNA, they were not significantly different in *LSL-KrasG12D/Pdx1-Cre* mice compared with the wild-type mice. Thus, the aberrant Hedgehog/GLI pathway is involved in chronic pancreatitis–carcinogenesis in *LSL-KrasG12D/Pdx1-Cre* mice. These results further support the findings that oncogenic *Kras* through the RAF/MEK/MAPK pathway suppresses GLI1 protein degradation and consequently play an important role in activating the Hedgehog signaling pathway (44). Secondly, the mice fed with capsaicin showed a significant downregulation of Shh and GLI1, implying targeting Hedgehog/GLI pathway by capsaicin could be a mechanism for inhibiting fibrosis in chronic pancreatitis.

Taken together, our results indicate that in the LSL-Kras^{G12D}/*Pdx1*-Cre mouse model, capsaicin demonstrates strong activities against inflammation and proliferation in the context of chronic pancreatitis and can inhibit progression of mPanIN lesions and carcinogenesis by blocking phospho-EKR and Hedgehog/GLI pathway activation. These results imply that capsaicin is a very promising agent for inhibiting chronic pancreatitis and mPanINs formation and ultimately pancreatic carcinogenesis.

Funding

National Institutes of Health (CA129038 to S.K.S. and CA122514 to G.Y.Y.).

Conflict of Interest Statement: None declared.

References

1. Whitcomb,D.C. (2004) Inflammation and Cancer V. Chronic pancreatitis and pancreatic cancer. *Am. J. Physiol. Gastrointest. Liver. Physiol.*, **287**, G315–G319.
2. Hussain,S.P. *et al*. (2003) Radical causes of cancer. *Nat. Rev. Cancer.*, **3**, 276–285.
3. Hermanova,M. *et al*. (2008) Expression of COX-2 is associated with accumulation of p53 in pancreatic cancer: analysis of COX-2 and p53 expression in premalignant and malignant ductal pancreatic lesions. *Eur. J. Gastroenterol. Hepatol.*, **20**, 732–739.
4. Whitcomb,D. *et al*. (2009) Germ-line mutations, pancreatic inflammation, and pancreatic cancer. *Clin. Gastroenterol. Hepatol.*, **7**, S29–S34.
5. Papoiu,A.D. *et al*. (2010) Topical capsaicin. The fire of a 'hot' medicine is reignited. *Expert Opin. Pharmacother.*, **11**, 1359–1371.

6. Caterina,M.J. *et al*. (1997) The capsaicin receptor: a heat-activated ion channel in the pain pathway. *Nature*, **389**, 816–824.
7. Yang,X. *et al*. (2010) Similar and different effects of capsaicin and resiniferatoxin on substance P release and transient receptor potential vanilloid type 1 expression of cultured rat dorsal root ganglion neurons. *Methods Find. Exp. Clin. Pharmacol.*, **32**, 3–11.
8. Thoennissen,N.H. *et al*. (2010) Capsaicin causes cell-cycle arrest and apoptosis in ER-positive and -negative breast cancer cells by modulating the EGFR/HER-2 pathway. *Oncogene*, **29**, 285–296.
9. Han,S.S. *et al*. (2001) Capsaicin suppresses phorbol ester-induced activation of NF-kappaB/Rel and AP-1 transcription factors in mouse epidermis. *Cancer Lett.*, **164**, 119–126.
10. Bhutani,M. *et al*. (2007) Capsaicin is a novel blocker of constitutive and interleukin-6-inducible STAT3 activation. *Clin. Cancer Res.*, **13**, 3024–3032.
11. Malagarie-Cazenave,S. *et al*. (2009) Capsaicin, a component of red peppers, induces expression of androgen receptor via PI3K and MAPK pathways in prostate LNCaP cells. *FEBS Lett.*, **583**, 141–147.
12. Maity,R. *et al*. (2010) Capsaicin induces apoptosis through ubiquitin-proteasome system dysfunction. *J. Cell. Biochem.*, **109**, 933–942.
13. Brown,K.C. *et al*. (2010) Capsaicin displays anti-proliferative activity against human small cell lung cancer in cell culture and nude mice models via the E2F pathway. *PLoS One*, **5**, e10243.
14. Hwang,J.T. *et al*. (2009) Anti-inflammatory and anticarcinogenic effect of genistein alone or in combination with capsaicin in TPA-treated rat mammary glands or mammary cancer cell line. *Ann N Y Acad Sci.*, **1171**, 415–420.
15. Babbar,S. *et al*. (2010) Inhibition and induction of human cytochrome P450 enzymes in vitro by capsaicin. *Xenobiotica*, **40**, 807–816.
16. Zhang,R. *et al*. (2008) In vitro and in vivo induction of apoptosis by capsaicin in pancreatic cancer cells is mediated through ROS generation and mitochondrial death pathway. *Apoptosis*, **13**, 1465–1478.
17. Anandakumar,P. *et al*. (2009) Chemopreventive task of capsaicin against benzo(a)pyrene-induced lung cancer in Swiss albino mice. *Basic Clin. Pharmacol. Toxicol.*, **104**, 360–365.
18. Zhang,Z. *et al*. (1997) Effects of orally administered capsaicin, the principal component of capsicum fruits, on the in vitro metabolism of the tobacco specific nitrosamine NNK in hamster lung and liver microsomes. *Anticancer Res.*, **17**, 1093–1098.
19. Ji,B. *et al*. (2009) Ras activity levels control the development of pancreatic diseases. *Gastroenterology*, **137**, 1072–1082, 1082e1–e6.
20. Grippo,P.J. *et al*. (2005) Modeling pancreatic cancer in animals to address specific hypotheses. *Methods Mol. Med.*, **103**, 217–243.
21. Leach,S.D. (2004) Mouse models of pancreatic cancer: the fur is finally flying!. *Cancer Cell*, **5**, 7–11.
22. Jackson,E.L. *et al*. (2001) Analysis of lung tumor initiation and progression using conditional expression of oncogenic K-ras. *Genes Dev.*, **15**, 3243–3248.
23. Johnson,L. *et al*. (2001) Somatic activation of the K-ras oncogene causes early onset lung cancer in mice. *Nature*, **410**, 1111–1116.
24. Hingorani,S.R. *et al*. (2003) Preinvasive and invasive ductal pancreatic cancer and its early detection in the mouse. *Cancer Cell*, **4**, 437–450.
25. Guerra,C. *et al*. (2007) Chronic pancreatitis is essential for induction of pancreatic ductal adenocarcinoma by K-Ras oncogenes in adult mice. *Cancer Cell*, **11**, 291–302.
26. Willemer,S. *et al*. (1992) Hormone-induced pancreatitis. *Eur. Surg. Res.*, **24** (suppl. 1), 29–39.
27. Yoo,B.M. *et al*. (2005) Novel antioxidant ameliorates the fibrosis and inflammation of cerulein-induced chronic pancreatitis in a mouse model. *Pancreatology*, **5**, 165–176.
28. Schmidt,R.A. *et al*. (1984) Evidence for post-translational incorporation of a product of mevalonic acid into Swiss 3T3 cell proteins. *J. Biol. Chem.*, **259**, 10175–10180.
29. Hingorani,S.R. *et al*. (2005) Trp53R172H and KrasG12D cooperate to promote chromosomal instability and widely metastatic pancreatic ductal adenocarcinoma in mice. *Cancer Cell*, **7**, 469–483.
30. Ulmasov,B. *et al*. (2010) Angiotensin II signaling through the AT1a and AT1b receptors does not have a role in the development of cerulein-induced chronic pancreatitis in the mouse. *Am. J. Physiol. Gastrointest. Liver Physiol.*, **299**, G70–G80.
31. Hruban,R.H. *et al*. (2001) Pancreatic intraepithelial neoplasia: a new nomenclature and classification system for pancreatic duct lesions. *Am. J. Surg. Pathol.*, **25**, 579–586.
32. Seril,D.N. *et al*. (2002) Inhibition of chronic ulcerative colitis-associated colorectal adenocarcinoma development in a murine model by N-acetylcysteine. *Carcinogenesis*, **23**, 993–1001.
33. Rivera,J.A. *et al*. (1997) Analysis of K-ras oncogene mutations in chronic pancreatitis with ductal hyperplasia. *Surgery*, **121**, 42–49.
34. Oyagbemi,A.A. *et al*. (2010) Capsaicin: a novel chemopreventive molecule and its underlying molecular mechanisms of action. *Indian J. Cancer,*, **47**, 53–58.
35. Seril,D.N. *et al*. (2003) Oxidative stress and ulcerative colitis-associated carcinogenesis: studies in humans and animal models. *Carcinogenesis*, **24**, 353–362.
36. Roncucci,L. *et al*. (2008) Myeloperoxidase-positive cell infiltration in colorectal carcinogenesis as indicator of colorectal cancer risk. *Cancer Epidemiol. Biomarkers Prev.*, **17**, 2291–2297.
37. Hruban,R.H. *et al*. (2006) Pancreatic cancer in mice and man: the Penn Workshop 2004. *Cancer Res.*, **66**, 14–17.
38. Iatropoulos,M.J. *et al*. (1996) Proliferation markers. *Exp. Toxicol. Pathol.*, **48**, 175–181.
39. Niault,T.S. *et al*. (2010) Targets of Raf in tumorigenesis. *Carcinogenesis*, **31**, 1165–1174.
40. Mebratu,Y. *et al*. (2009) How ERK1/2 activation controls cell proliferation and cell death: is subcellular localization the answer? *Cell Cycle*, **8**, 1168–1175.
41. Shek,F.W. *et al*. (2002) Expression of transforming growth factor-beta 1 by pancreatic stellate cells and its implications for matrix secretion and turnover in chronic pancreatitis. *Am. J. Pathol.*, **160**, 1787–1798.
42. Luttenberger,T. *et al*. (2000) Platelet-derived growth factors stimulate proliferation and extracellular matrix synthesis of pancreatic stellate cells: implications in pathogenesis of pancreas fibrosis. *Lab. Invest.*, **80**, 47–55.
43. Bailey,J.M. *et al*. (2008) Sonic hedgehog promotes desmoplasia in pancreatic cancer. *Clin. Cancer Res.*, **14**, 5995–6004.
44. Ji,Z. *et al*. (2007) Oncogenic KRAS activates hedgehog signaling pathway in pancreatic cancer cells. *J. Biol. Chem.*, **282**, 14048–14055.

Received May 2, 2011; revised July 9, 2011; accepted August 8, 2011